

# Power Transformer Analytical Design Approaches

P.S. Bodger and S.C. Bell

Department of Electrical and Computer Engineering  
University of Canterbury

## Abstract

Conventional and reverse approaches to transformer design are presented in this paper. The first uses device ratings to determine the sizes of the core and windings. In the reverse approach, the physical characteristics and dimensions of the windings and core are the specifications. By manipulating the amount and type of material actually to be used in the construction of the transformer, its performance can be determined. Such an approach is essentially the opposite of the conventional transformer design method. Both design methods are applied to two sample high voltage transformers. The measured performances of the as-built transformers highlight the limitations in using the conventional method, which are overcome using the reverse approach.

## 1. INTRODUCTION

From a manufacturer's perspective it is convenient to design and produce a set range of transformer sizes. Usually, the terminal voltages, VA rating and frequency are specified. These specifications decide the materials to be used and their dimensions. This approach to transformer design has been utilised and presented in detail in textbooks [1,2]. It has been used as a design tool for teaching undergraduate power system courses at universities [3-5]. In addition, it has also been used extensively in designing switched mode power supplies [6,7]. Finite Element Analysis has also been applied, concurrent with the above approach, to aid the overall design process [8,9].

However, by designing to rated specifications, consideration is not explicitly given to what materials and sizes are actually available. Core and winding material suppliers offer catalogues of preferred sizes. This reflects the supplier's manufacturing capabilities in extrusion, rolling and forming tools and equipment. It is not economic to offer customers any size and shape they require. It is possible that an engineer, having designed a transformer, may then find the material sizes do not exist. The engineer may then be forced to use available materials. Consequently the performance of the actual transformer built is likely to be different from that of the design calculations.

In the reverse design approach, the physical characteristics and dimensions of the windings and core are the specifications. By manipulating the amount and type of material actually to be used in the transformer construction, its performance can be determined. Such an approach lends itself to designing transformers using what is available from suppliers. This is essentially the opposite of the conventional transformer design method. It allows for customised design, as there is considerable flexibility in meeting the performance required for a particular application.

This paper presents previous research in which both the conventional and reverse design approaches have been compared [10]. However, some anomalies have been corrected and the use of finite element analysis has been added to the reverse design approach.

## 2. CONVENTIONAL DESIGN

Consideration is given to the layout of the core and windings of a two winding transformer. The laminated core occupies the central space. The windings are wrapped around the core, with the low voltage (LV) winding inside the high voltage (HV) winding. Insulation is allowed for between the core and windings, between windings, around winding wire and in between each layer of winding if required.

The yokes and limbs of the core are additional to this. They depend on whether the transformer is a "core" or "shell" type [11] and have dimensions determined by the boundaries of the windings and cross-section of the core. Usually, for smaller transformers, the core laminations come in discrete sizes. For shell type cores they may be fabricated to eliminate waste from stamping from rolled strip. Such "scrapless" EI cores [12] have specific ratios for their window dimensions and magnetic path sizes.

In the conventional approach to designing transformers, the terminal voltages,  $V_1$ ,  $V_2$ , VA rating,  $S$ , and frequency,  $f$ , are specified. Material characteristics then lead to calculation of core and winding dimensions. Based on the designer's experience, core steel with known relative permeability,  $\mu_r$ , and knee point flux density,  $B$ , is chosen. A stacking factor,  $SF_c$ , is assigned to account for the lamination's metal and insulation composition. A window width factor,  $WWF$ , (the ratio of winding space height to width) is also selected, again on experience.

For the primary and secondary windings, acceptable current densities,  $J_1, J_2$ , volts per turn,  $VT_1, VT_2$ , and space factors,  $SF_1, SF_2$  (amount of copper to winding cross-sectional area) are chosen. The current density estimates are made based on generally accepted thermal capacities of transformer winding material. Typically this is 1-2 A/mm<sup>2</sup> for copper or aluminium.

The volts per turn reflect a designer's experience and may differ from one manufacturer to another. In practice the values vary from under unity to more than 50, with inside this range being most typical. An empirical formula cited in the literature [11] is

$$VT = \frac{\sqrt{S}}{VTF} \quad (1)$$

where:

$VTF$  = voltage per turn factor

All this achieves is to move the problem of estimating the volts per turn to the factor. No calculation is presented for the latter.

The space factors depend on voltage ratings and the insulation systems used. It is difficult to find any general rules for specifying this. Again experience determines the values. An estimate can be gained by considering the amount of winding area in the total area enclosed by the centres of four adjacent turns.

Having specified the ratings and made estimates of the other factors listed above, the design procedure for the transformer then follows a more calculated path. The current ratings are

$$I_1 = \frac{S}{V_1}, \quad I_2 = \frac{S}{V_2} \quad (2)$$

Hence the areas of the winding wires are

$$A_1 = \frac{I_1}{J_1}, \quad A_2 = \frac{I_2}{J_2} \quad (3)$$

Thicknesses,  $t_1$  and  $t_2$ , can be calculated for circular cross-section wires from

$$t_1 = \sqrt{\frac{4A_1}{\pi}}, \quad t_2 = \sqrt{\frac{4A_2}{\pi}} \quad (4)$$

From the chosen volts per turn, the number of turns per winding is

$$N_1 = \frac{V_1}{VT_1}, \quad N_2 = \frac{V_2}{VT_2} \quad (5)$$

from which the winding turns ratio is

$$a = \frac{N_1}{N_2} \quad (6)$$

This is only the same as the voltage ratio if the volts per turn are the same for both windings.

From the 'Transformer Equation' [13]

$$V_1 = 4.44N_1f\phi \quad (\phi = BA'_c) \quad (7)$$

The area of the core can be calculated from

$$A'_c = \frac{V_1}{4.44N_1fB} \quad (8)$$

The actual core dimensions include the stacking factor.

$$A_c = \frac{A'_c}{SF_c} \quad (9)$$

The winding window areas are calculated from

$$A_{w1} = \frac{N_1A_1}{SF_1} \quad (10)$$

$$A_{w2} = \frac{N_2A_2}{SF_2} \quad (11)$$

The winding window width and height are

$$WW = \sqrt{\frac{A_{w1} + A_{w2}}{WWF}} \quad (12)$$

$$WH = WWF * WW \quad (13)$$

### 3. REVERSE TRANSFORMER DESIGN

A transformer profile showing known material characteristics and dimensions is depicted in Fig. 1. In the reverse design method, the transformer is built up from the core outwards. The core cross-section dimensions (diameter for a circular core and side lengths for a rectangular core) are selected from catalogues of available materials. A core length is chosen. Laminations that are available can be specified in thickness. A core stacking factor can be estimated from the ratio of iron to total volume.

The winding and core material resistivities and permeabilities become specifications.

Given the core length,  $l_c$ , and diameter, DC (or  $b_{core}$  and  $w_{core}$  for a rectangular core), the inside winding (usually the low voltage winding) is wound on layer by layer. The wire size can be selected from catalogues. They also specify insulation thickness. The designer can then specify how many layers of each winding are wound.

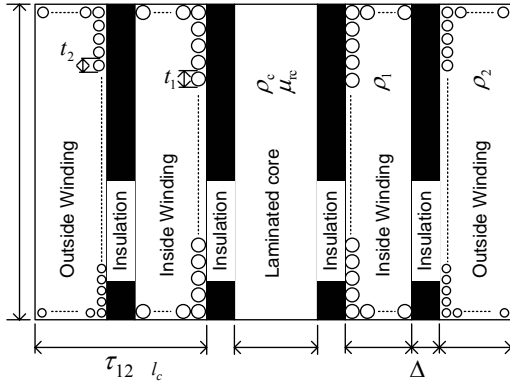


**Fig. 1.** Centre limb of a transformer showing component dimensions and material properties.

Insulation is placed between the core and the inside winding (former) and between each layer for high voltage applications. Insulation can also be placed between each winding. The outer winding (usually the HV winding) is wound over the inside winding, with insulation between layers according to the voltage between them.

Instead of ‘guessing’ the values of  $SF_1$ ,  $SF_2$  and  $WWF$ , as required in the conventional approach, these can be accounted for by knowledge of the actual dimensions of materials used. Also winding current densities and volts per turn become a consequence of the design, rather than a design specification.

The only rating requirements are the primary voltage and frequency. The secondary voltage and transformer VA rating are a consequence of the construction of the transformer.

The number of turns on the windings are estimated to be:

$$N_1 = \frac{L_1 l_c}{t_1}, \quad N_2 = \frac{L_2 l_c}{t_2} \quad (14)$$

where:

- $L_1$  = number of primary winding layers
- $L_2$  = number of secondary winding layers
- $l_c$  = length of the core

This calculation assumes that the winding length is equal to the core length. The core length may be substituted for actual winding lengths if the primary and secondary winding lengths are different or if the windings do not fully occupy the winding window height.

## 4. EQUIVALENT CIRCUIT MODELS

For either design approach, the equivalent circuit shown in Fig. 2 is often used to represent the transformer at supply frequencies [13].

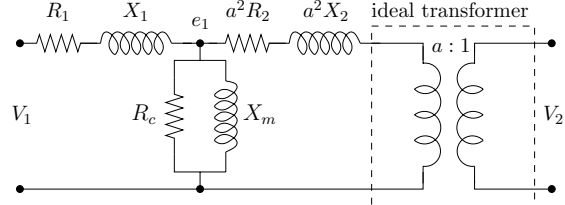


**Fig. 2.** Transformer equivalent circuit, referred to the primary winding.

Each component of the equivalent circuit can be calculated from the transformer material characteristics and dimensions.

### 4.1 Resistance Models

#### 4.1.1 Core loss Resistance

The losses in the core consist of two major components; the hysteresis loss and the eddy current loss. The hysteresis loss can be calculated using [13]

$$P_h = k_h f B^x W T \quad (15)$$

where:

- $k_h$  = constant depending on the material, typically 0.11
- $x$  = Steinmetz factor, typically 1.85
- $WT$  = weight of core

The eddy current loss is expressed as [14]

$$P_{ec} = \frac{c_l^2}{12 \rho_c} \frac{l_c}{N_1^2 A_c} e_1^2 k_v \quad (16)$$

where:

- $c_l$  = lamination thickness
- $\rho_c$  = operating resistivity of the core
- $A_c$  = cross-sectional area of the core
- $e_1^2$  = induced primary winding voltage
- $k_v$  = total core volume / central limb volume

The variation of resistivity with temperature should be accounted for, since the transformer will be heated up under operation. The operating resistivity at temperature  $T^\circ\text{C}$  is

$$\rho = \rho_{c-20^\circ\text{C}} (1 + \Delta \rho (T_c - 20)) \quad (17)$$

where:

$\Delta\rho_c$  = thermal resistivity coefficient  
 $\rho_{c-20^\circ\text{C}}$  = material resistivity at 20°C

$$R_2 = \frac{\rho_2 l_2}{A_2} \quad (21)$$

The hysteresis and eddy current losses can be expressed in terms of the induced voltage  $e_1$  as

$$P_h = \frac{e_1^2}{R_h}, \quad P_{ec} = \frac{e_1^2}{R_{ec}} \quad (18)$$

where:

$R_h$  = hysteresis loss equivalent resistance  
 $R_{ec}$  = eddy current loss equivalent resistance

Thus, both  $R_h$  and  $R_{ec}$  can be included in the model as the core loss resistance  $R_c$ .  $R_c$  is expressed as

$$R_c = \frac{R_h R_{ec}}{R_h + R_{ec}} \quad (19)$$

#### 4.1.2 Primary Winding Resistance

The primary winding resistance is

$$R_1 = \frac{\rho_1 l_1}{A_1} \quad (20)$$

where:

$\rho_1$  = resistivity of the primary winding wire  
 $l_1$  = effective length of the wire  
 $A_1$  = cross-sectional area of the wire

The resistivity is temperature dependent and should be adjusted according to Eq. 17. In the reverse design method the effective length of the primary winding wire is estimated by calculating the length of wire on each layer of the winding, and then summing over all layers, taking into account the increasing diameter of each layer wound around the previous one.

The winding space factors, present in the conventional design method, give no indication of the actual distribution of turns over the winding space. There is no guarantee that an integer number of layers will fit in the calculated winding width. Consequently the as-built transformer may contain less turns than calculated, even if the above space factors are correct. The effective length of the primary winding wire is estimated from a mean radial length, equal to the radial distance from the core centre to one quarter of the winding window.

#### 4.1.3 Secondary Winding Resistance

The secondary winding resistance is

where:

$\rho_2$  = resistivity of the secondary winding wire  
 $l_2$  = effective length of the wire  
 $A_2$  = cross-sectional area of the wire

The effective length of the secondary winding wire is calculated in a similar manner to that for the primary winding wire for the reverse design method. In the conventional design method this is estimated from a mean radial length, equal to the radial distance from the core centre to three quarters of the winding window. As for the primary winding, the resistivity is adjusted for the operating temperature.

## 4.2 Inductive Reactance Models

### 4.2.1 Magnetising Reactance

The magnetising reactance is [15]

$$X_m = \frac{\omega N_1^2 \mu_o \mu_{rc} A_c}{l_{eff}} \quad (22)$$

where:

$l_{eff}$  = effective path length for mutual flux  
 $\mu_o$  = permeability of free space ( $4\pi \times 10^{-7} \text{Hm}^{-1}$ )  
 $\mu_{rc}$  = relative permeability of core  
 $\omega$  =  $2\pi f$

### 4.2.2 Primary and Secondary Leakage Reactances

The primary and secondary leakage reactances are assumed to be the same, when referred to the primary, and are each half of the total transformer leakage reactance. One form of expression is: [16]

$$X_1 = a^2 X_2 = \frac{1}{2} \frac{\mu_o N_1^2}{l_c} \left( \frac{\bar{l}_p d_1 + \bar{l}_s d_2}{3} + \bar{l}_{ps} \Delta d \right) \quad (23)$$

where:

$\bar{l}_p, \bar{l}_s$  = mean circumferential length of primary and secondary windings  
 $\bar{l}_{ps}$  = mean circumferential length of interwinding space  
 $d_1, d_2$  = thickness of primary and secondary windings (see Fig. 1)  
 $\Delta d$  = thickness of interwinding space

Having obtained the component values, the equivalent circuit can be solved. Open circuit, short circuit and loaded circuit performances can be estimated by putting an impedance  $Z_L = R_L + jX_L$  across the output and varying its value. Further, performance measures of voltage regulation and power transfer efficiency for any load condition can be readily calculated. Current flows and densities in the windings can be calculated and compared to desired levels.

## 5. COMPARISON OF APPROACHES – TWO DESIGN EXAMPLES

To illustrate the two approaches to transformer design, two single-phase, 50 Hz, high voltage transformers have been designed, built and tested. Their nominal ratings are listed in Table I.

TABLE I  
Nominal ratings of high voltage transformers

Transformer	#1	#2
Primary voltage (V)	240	14
Secondary voltage (kV)	6.24	4.56
VA rating (VA)	200	617

Transformer #1 was designed for the power supply of an electric water purification device [17]. Transformer #2 was a model, designed to evaluate the harmonic performance of capacitive voltage transformers. Both transformers were built as shell types with rectangular cores. The transformers were for special applications and not procurable directly from a manufacturer.

### 5.1 Conventional design approach

The transformers were first designed using the conventional approach. In addition to the rating data above, estimates of the core maximum flux density, stacking factors, current densities, volts per turn factors, and the winding width factor were specified, as listed in Table II.

Standard physical values of material permeabilities, resistivities and thermal resistivity coefficients were also entered as data, for the core steel and copper windings, as shown in Table III. The two transformers were constructed using different core steel but the equivalent circuit models in this paper do not account for this. A core stacking factor of 0.95 was estimated for both transformers.

The dimensions of the core and winding window were calculated, along with an estimate of the number of primary and secondary turns. This is shown in Table IV.

TABLE II  
Data for conventional transformer design

Transformer	#1	#2
Primary voltage (V)	240	14
<b>Core:</b>		
Peak flux density (T)	1.5	1.65
Window width factor	3	5
<b>LV winding:</b>		
Current density (A/mm <sup>2</sup> )	2	3
Voltage per turn factor	24	49
Space factor	0.35	0.5
<b>HV winding:</b>		
Current density (A/mm <sup>2</sup> )	2	3
Voltage per turn factor	24	49
Space factor	0.35	0.5

TABLE III  
Material constants

	Core	LV Winding	HV Winding
Rel. permeability:	3000	1	1
Resistivity at 20°C (Ωm)	$1.8 \times 10^{-7}$	$1.76 \times 10^{-8}$	$1.76 \times 10^{-8}$
Thermal resistivity coeff. (°C)	0.006	0.0039	0.0039
Operating temperature (°C)	50	50	50
Density (kg/m <sup>3</sup> )	7870	8960	8960

TABLE IV  
Dimensions obtained using conventional transformer design method

Transformer	#1	#2
<b>Core:</b>		
Length (mm)	54	90
Width 1 (mm)	43	38
Width 2 (mm)	43	38
<b>Window:</b>		
Width (mm)	18	18
Height (mm)	54	90
<b>LV winding:</b>		
Wire diameter (mm)	0.73	4.3
Number of turns	407	27
<b>HV winding:</b>		
Wire diameter (mm)	0.14	0.24
Number of turns	10590	8995

### 5.2 Reverse design approach

Once the transformer designs had been obtained using the conventional approach, consideration was given to the wire gauges, insulation material, and core dimensions that were actually available. For Transformer #2, the available core dimensions were

significantly different than the calculated values. The actual dimensions of the various components that were to be used to construct the transformers were entered as data for the reverse transformer design method, shown in Table V

TABLE V  
Data for reverse transformer design method

Transformer	#1	#2
<b>Core:</b>		
Length (mm)	68	114
Width 1 (mm)	51	152
Width 2 (mm)	44	44
Core/LV insulation thickness (mm)	2	3.25
<b>LV winding:</b>		
Length	66	114
Number of layers	5	1
Wire diameter (mm)	0.8	3.55
Interlayer insulation thickness (mm)	0.5	0
LV/HV insulation thickness (mm)	0.7	6.5
<b>HV winding:</b>		
Length	66	114
Number of layers	20	20
Wire diameter (mm)	0.125	0.212
Interlayer insulation thickness (mm)	0.5	0.09

Using the reverse design approach, only the frequency and nominal primary voltage are entered as rated data.

The number of layers of wire on the primary and secondary windings was determined using an iterative design procedure. The initial number of layers was estimated by matching the winding thickness to the winding window width calculated using the conventional design method. Next, the performance was calculated at rated conditions and compared to the nominal specifications. The number of primary and secondary layers was then modified to obtain a better match with the nominal specifications.

### 5.3 Calculated and Measured Performances

#### 5.3.1 Equivalent circuit parameters

The equivalent circuit parameters, referred to the primary, calculated for the transformers using both conventional and reverse design methods, along with the measured values, as determined by open circuit and short circuit tests, are presented in Table VI.

The reverse transformer design method more accurately calculated the winding resistance and leakage reactance values for the sample transformers. This is because the geometry of the transformer models better matches that of the actual transformers.

TABLE VI  
Calculated and measured equivalent circuit parameters for sample transformers

Equi. Circuit Params.	#1			#2		
	Conv.	Revr.	Meas.	Conv.	Revr.	Meas.
$R_c(\Omega)$	1380	1342	3388	3.9	9.9	18
$X_m(\Omega)$	1380	1383	1987	4.0	11.9	41
$R_{wind}(\Omega)$	7.8	11.5	10.0	0.014	0.055	0.043
$X_{leak}(\Omega)$	1.5	1.9	2.8	0.004	0.016	0.012

Neither of the two approaches accurately calculates the magnetising reactance. This highlights the limitations of the simple linear model. The non-linear anisotropic magnetic properties of the core steel and the core construction details are not taken into account.

The conventional transformer design method predicts much higher losses than the reverse transformer design method for Transformer #2. This is due to an overestimation of the magnetic flux density, which occurred because the transformer core was constructed with different dimensions than the calculated values.

These results show that the reverse design method, with its particular accounting of actual dimensions, most accurately models the equivalent circuit parameters.

### 5.4 Load tests

A resistance was placed across the secondary of Transformer #1 to obtain the rated load conditions at unity power factor. The model performance was calculated by adjusting the load resistance so that the calculated secondary VA matched the measured value. On the other hand, since Transformer #2 was designed for capacitive loads, an open circuit condition was used to compare calculated and measured values. The results are listed in Table VII.

TABLE VII  
Calculated and measured rated load performance

	#1			#2		
	Conv.	Revr.	Meas.	Conv.	Revr.	Meas.
$V_1(\text{V})$	240	240	240	14.05	14.05	14.05
$I_1(\text{A})$	0.90	0.91	0.76	5.0	1.8	1.0
$V_2(\text{kV})$	6.1	5.9	6.2	4.6	4.7	4.6
$I_2(\text{mA})$	28	28	27	0	0	0
$P_1(\text{W})$	213	216	181	50	20	8
Effy.(%)	79	77	92	0	0	0
Reg.(%)	2.6	3.8	0.7	0.2	0.3	0.1

The values listed in Table VII show that despite the variation in equivalent circuit parameter estimation, both the conventional and the reverse design methods give performance results which are useful in predicting the actual performance of as-built transformers.

Usually, the load on a transformer in operation varies so the design is most about size and ultimate ratings. Either of the approaches can be taken depending on the limitations present.

## 6. INCORPORATING FINITE ELEMENT MODELLING INTO THE REVERSE DESIGN METHOD

### 6.1 Introduction

The reverse design method calculated the performance of the two sample transformers more accurately than the conventional design method. It allows for a more accurate estimate to be made of the geometry of the as-built transformer at the design stage. However, both models are limited to the accuracy of the equivalent circuit parameters.

In this section a magnetostatic finite element model is introduced as an alternative method for calculating the reactance components of the equivalent circuit model. Basic two- and three-dimensional models are developed which improve on the accuracy of the traditional methods, provide a graphical view of the transformer magnetic fields, and provide a foundation for more advanced models.

### 6.2 Transformer design program

A transformer design program, based on the reverse design method, was written in a MS Excel workbook. The workbook contains a main worksheet, several input and output worksheets and several modules, written in Visual Basic for Applications (VBA) code. One module was used to couple the workbook to the commercial finite element analysis software package MagNet [18]. By automating the process of finite element modelling, much time is saved and the likelihood of user error is reduced.

### 6.3 Model detail

Each winding was modelled as a single block of non-magnetic material encompassing all turns over all layers. Uniform current density was assumed. The core was modelled as a single non-conducting isotropic material of constant relative permeability. Any eddy currents induced in the windings and core were assumed to have a negligible affect on transformer performance. This assumption was enforced by using a static solver. The transformer was

enclosed by a rectangular air-space with dimensions twice that of the core, to which a tangential flux boundary condition was applied. The default mesh was automatically refined using the in-built h-adaptation feature and the solution polynomial order was set to 3.

Solving time was reduced for the three-dimensional model by making use of transformer symmetry. Only 1/8<sup>th</sup> of the transformer was modelled. The model geometry for Transformer #1, along with the initial mesh, is shown in Fig. 3.

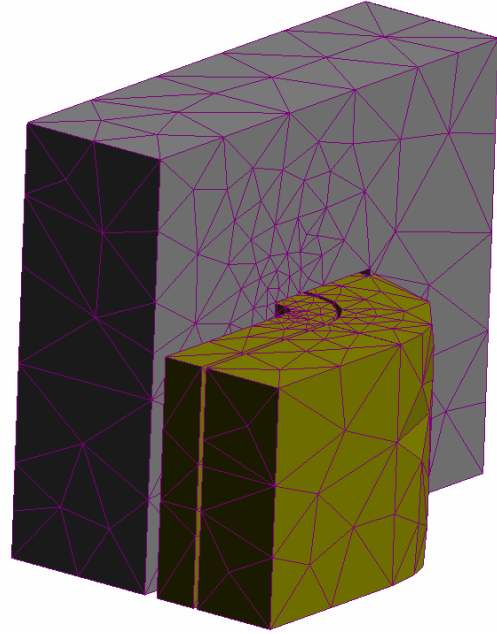


**Fig. 3:** Transformer #1 geometry for the three-dimensional model, including initial mesh (air space mesh not shown).

### 6.4 Reactance calculations

The winding inductances are defined as [19]

$$L_{ij} = N_i N_j P_{ij} \quad (24)$$

where:

$N_i, N_j$  is the number of turns on winding  $i$  and  $j$

$P_{ij}$  is the magnetic permeance, defined as

$$P_{ij} = \frac{\lambda_i}{i_j} \quad (25)$$

$\lambda_i$  is the flux-linkage of winding  $i$  due to an excitation current in winding  $j$ .

The three magnetic permeances of the two-winding transformer,  $P_{11}$ ,  $P_{12}$ , ( $= P_{21}$ ) and  $P_{22}$ , are calculated in two simulations.

The winding self- and mutual-inductances are converted into components of a T equivalent circuit. Together with the core and winding resistances, this forms the transformer equivalent circuit of Fig. 2. The reactance values are given by

$$X_m = a\omega L_{12} \quad (26)$$

$$X_1 = \omega L_{11} - a\omega L_{12} \quad (27)$$

$$a^2 X_2 = a^2 \omega L_{22} - a\omega L_{12} \quad (28)$$

### 6.5 Alternative calculation of leakage reactances

An alternative method of calculating the leakage reactance is based on energy techniques [20]. This provides a simple calculation check, and is less prone to numerical errors than the self- and mutual inductance method, where the (typically small) value of leakage inductance is given by the difference between two large numbers [21]. However, the alternative method cannot resolve the individual leakage reactance values. For transformers with different primary and secondary winding lengths, or incomplete magnetic cores, the common assumption that the leakage reactances are equal when referred to the primary is no longer valid [22].

The total leakage reactance referred to the primary winding is computed from the calculated total stored energy  $W_s$ . The number of primary and secondary turns are both set to  $N_1$ , the primary winding is energised with current  $+i_s$  and the secondary winding is energised with current  $-i_s$ . The leakage reactance is given by:

$$X_1 + a^2 X_2 = \frac{2\omega W_s}{i_s^2} \quad (29)$$

### 6.6 Results

The reactance components of the two transformers calculated using two- and three-dimensional finite element models are compared to the existing model and the measured results in Table VIII.

The finite element model calculated higher values of magnetising reactance than the existing model. This can be explained by considering the open-circuit magnetic field plot of Fig. 4. The magnetic flux plot essentially shows the transformers' mutual flux since the primary leakage is negligible under open-circuit conditions. With this linear model, the flux density is greatest at the inside edges of the core, where the

TABLE VIII  
Model and measured reactance values

	Transformer #1		Transformer #2	
	$X_m(\Omega)$	$X_{leak}(\Omega)$	$X_m(\Omega)$	$X_{leak}(\Omega)$
Existing	1383	1.9	11.9	0.016
2D FEM	1905	0.6	18.8	0.003
3D FEM	1898	1.6	18.9	0.015
Meas.	1987	2.8	41.0	0.012

highest calculated value exceeds 7.5T, highlighting the limitations of the static model. The effect is to reduce the effective path length of the magnetic flux, thereby increasing the magnetising reactance.

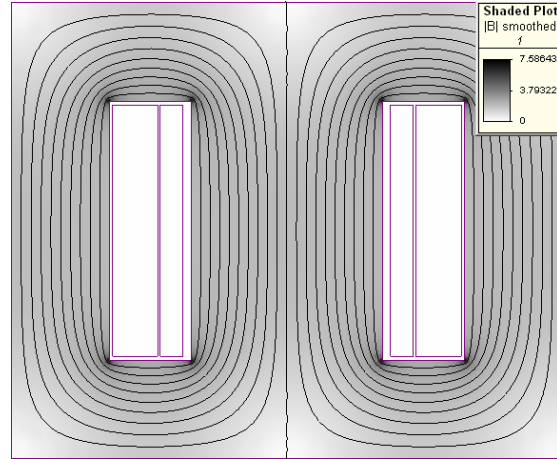
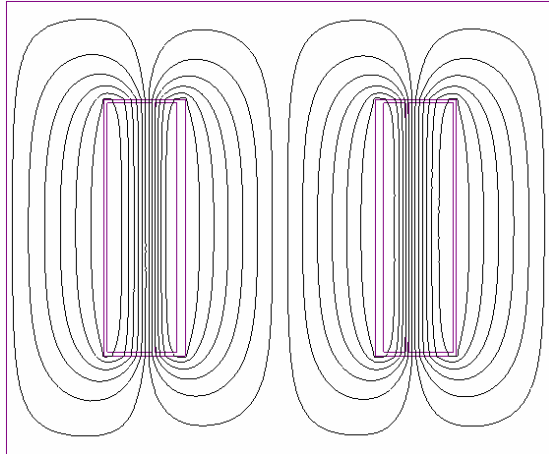


Fig. 4: Field plot of Transformer #1 under open-circuit conditions using a linear 2D magnetostatic finite element model.

The two-dimensional finite element model underestimates the leakage reactance because the end-winding field is neglected. The three-dimensional model gives similar results to the existing model. The mismatch between model and measured results for Transformer #1 may be attributed to the differences in geometry between the designed and as-built transformer.

The two-dimensional magnetic field plot of Transformer #1 under short-circuit conditions is shown in Fig. 5. The flux-density is highest in the centre of the winding region and is approximately uniform. Fringing occurs near the top and bottom of the windings, and the flux density falls to negligibly low values once inside the core. This explains why classical techniques for calculating leakage reactance can be highly accurate even though they neglect fringing effects and assume a zero reluctance return path back through the core.



**Fig. 5:** Field plot of Transformer #1 under short-circuit conditions using a linear 2D magnetostatic finite element model.

### 6.7 Non-linear core model

Using a three-dimensional linear finite element model, a reasonable match was obtained between test and model results for the two sample transformers. However, for detailed analysis, a non-linear core model is required.

Transformer #1 was re-modelled using the in-built non-linear, non-oriented, core steel material M19. Magnetostatic simulation of the open-circuit test is more difficult with a non-linear core model. The magnetising current and flux density become non-linear functions of the applied voltage, but the primary voltage cannot be directly specified as the solver is current driven.

Using an iterative procedure, the peak magnetic field for Transformer #1 was calculated under open circuit conditions. The primary current was adjusted until its product with the magnetising reactance was equal to the peak value of primary voltage. The resulting field, shown in Fig. 6, more closely resembles the operating flux density. The peak flux density throughout most of the core is about 1.2T, matching the value calculated using the ‘transformer equation’ (7).

The core relative permeability for Transformer #1 was calculated at the instant in time where the magnetic field peaked. This is shown in Fig 7. At this time, the magnetising reactance was calculated to be 1884Ω. This is in close agreement to the previously calculated value of 1905Ω, obtained using a linear model with relative permeability of 3000. Fig. 7 may also explain why the linear model under-estimated the magnetising reactance of Transformer #2. The open-circuit test was performed at a reduced flux density, where the effective relative permeability is higher.

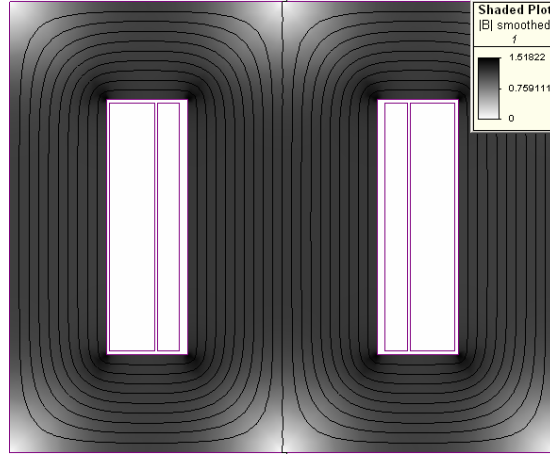


**Fig. 6:** Field plot of Transformer #1 under open-circuit conditions using a non-linear core model.

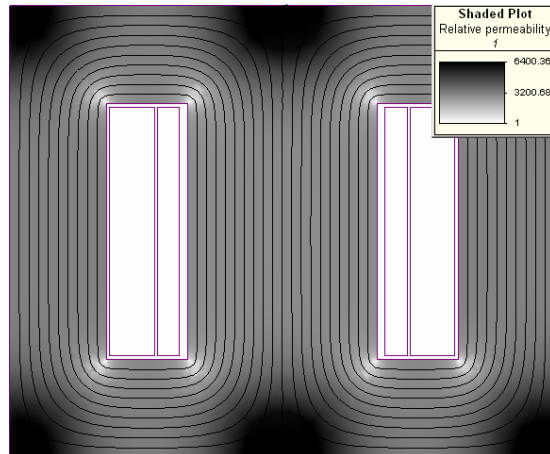


**Fig. 7:** Core relative permeability of Transformer #1 under open-circuit conditions.

More advanced models account for the anisotropic properties of the core and the core construction details. B-H curves and loss data, measured in both the rolling and traverse directions, can be incorporated into the finite element model. Such models are currently used in industry for highly accurate calculation of core losses [23].

## 7. CONCLUSIONS

Conventional transformer design starts from a consideration of required frequency, voltage and VA ratings. It estimates a number of factors for the core and winding arrangement, using values that are generally only known to experienced design engineers. The resultant design may not match what is actually available in materials and hence the predicted performance can be in error.

An alternative is to reverse the design procedure. The dimensions of core and winding materials are entered based on what is available. The overall size, ratings

and performance of the transformer can then be predicted.

Sample high voltage transformers have been designed, built and tested. The results highlight the problems associated with the conventional design and show the usefulness of the reverse design approach. Such a design philosophy allows for the exploration in the design of transformers with alternative construction options, where flexibility in shape and size is required.

## 8. REFERENCES

- [1] Lowdon, E., *Practical Transformer Design Handbook*, McGraw-Hill, Inc., 2nd edition, 1989.
- [2] McLyman, W.T., *Transformer and Inductor Design Handbook*, Dekker, New York, USA, 3rd edition, 2004.
- [3] Rubaai, A., "Computer aided instruction of power transformer design in the undergraduate power engineering class", *IEEE Trans. on Power Systems*, Aug 94, v. 9, No. 3, pp. 1174-1181.
- [4] Jewell, W.T., "Transformer design in the undergraduate power engineering laboratory", *IEEE Trans. on Power Systems*, May 90, v. 5, No. 2, pp. 499-505.
- [5] Shahzad, F., and Shwehdi, M.H., "Human-computer interaction of single/three phase transformer design and performance", *Industrial and Commercial Power Systems Technical Conference*, May 97, pp. 193-196.
- [6] Hurley, W.G., Wölfle, W.H. and Breslin, J.G., "Optimized transformer design: inclusive of high-frequency effects", *IEEE Trans. on Power Electronics*, July 98, v. 13, No. 4, pp. 651-659.
- [7] Petkov, R., "Design issues of high-power high-frequency transformer", *Proc. 1995 International Conference on Power Electronics and Drive Systems*, Feb 95, v. 1, pp. 401-410.
- [8] Asensi, R., Cobos, J.A., Garcia, O., Prieto, R., and Uceda, J., "A full procedure to model high frequency transformer windings", *IEEE Power Electronics Specialist Conference PESC'94*, June 94, v. 2, pp. 856-863.
- [9] Allcock, R., McClelland, R., Holland, S.A., and Roué, A., "Transformer design and analysis using finite element methods", *IEE Colloquium on Computation in Electrostatics*, 1995, pp. 8/1-8/3.
- [10] Bodger, P.S., Liew, M.C., and Johnstone, P.T., "A comparison of conventional and reverse transformer design", *Australasian Universities Power Engineering Conference (AUPEC)*, Brisbane, Australia, September 2000, pp. 80-85.
- [11] Slemon, G.R., and Straughen, A., *Electric Machines*, Addison-Wesley, Inc., USA, 1980.
- [12] Flanagan, W.M., *Handbook of Transformer Applications*, McGraw-Hill, 1986.
- [13] Paul, C.R., Nasar, S.A., and Unnewehr, L.E., *Introduction to Electrical Engineering*, McGraw-Hill, Inc., Singapore, 1986.
- [14] Slemon, G.R., *Magnetolectric Devices: Transducers, Transformers, and Machines*, John Wiley and Sons, Inc., USA, 1966.
- [15] Say, M.G., *Alternating Current Machines*, Longman Scientific & Technical, England, 1983.
- [16] Connelly, F.C., *Transformers: Their principles and design for light electrical engineers*, Sir issac Putman & Sons Ltd, London, 1965.
- [17] Johnstone, P.T., and Bodger, P.S., "High voltage disinfection of liquids", *IPENZ Trans.*, Nov 97, v. 24, No. 1, EMCh, pp. 30-35.
- [18] Infolytica, [www.infolytica.com](http://www.infolytica.com)
- [19] Ong, C. M., *Dynamic Simulation of Electric Machinery using Matlab / Simulink*, Prentice Hall, New Jersey, 1st edition.
- [20] Lindbolm, A., Isberg, J. and Bernhoff, H., "Calculating the coupling factor in a multilayer coaxial transformer with air core", *IEEE Trans. On Magnetics*, Nov 2004, v. 40, pp. 3244-3248.
- [21] Edwards, J. D., *An Introduction to MagNet for Static 2D Modelling*, Infolytica Corporation.
- [22] Margueron, X. and Keradec, J.-P., "Design of equivalent circuits and characterization strategy of n-input coupled inductors", *IEEE Transactions on Industry Applications*, Jan – Feb 07, v. 43, issue 1, pp. 14-22.
- [23] Mechler, G.F. and Girgis, R.S., "Calculation of spatial loss distribution in stacked power and distribution transformer cores", *IEEE Trans. on Power Delivery*, Apr 98, v. 13, no. 2, pp. 532-537.